

Supplementary material

Polydispersity stabilizes Biaxial Nematic Liquid Crystals

S. Belli¹, A. Patti², M. Dijkstra³, and R. van Roij¹

¹*Institute for Theoretical Physics, Utrecht University,
Leuvenlaan 4, 3584 CE Utrecht, The Netherlands*

²*Institute of Advanced Chemistry of Catalonia, CSIC, C/ Jordi Girona 18-26, 08034 Barcelona, Spain*

³*Soft Condensed Matter Group, Debye Institute for NanoMaterials Science,
Utrecht University, Princetonplein 5, 3584 CC Utrecht, The Netherlands*

I. DENSITY FUNCTIONAL THEORY

In the present work the orientational degrees of freedom of the particles are treated within the Zwanzig model [1], hence a particular orientation can be identified with a number $i = 1, \dots, 6$ (cf. Tab. S1).

i	L	W	T
1	x	y	z
2	z	x	y
3	y	z	x
4	x	z	y
5	y	x	z
6	z	y	x

TABLE S1. Enumeration of the orientational configurations of a hard cuboid within the Zwanzig model. Each configuration i is identified with the directions (x, y, z) along which the particle axes (L, W, T) are aligned.

According to density functional theory it is possible to express the free energy of a system as a functional of the single-particle density $\rho_i^\alpha(\mathbf{r})$ of particles with orientation i ($i = 1, \dots, 6$) belonging to species α ($\alpha = 1, \dots, M$) as [2]

$$\frac{\mathcal{F}[\rho]}{k_B T} = \int d\mathbf{r} \sum_{\alpha, i} \rho_i^\alpha(\mathbf{r}) \left[\ln(\rho_i^\alpha(\mathbf{r}) \Lambda_\alpha^3) - 1 \right] + \frac{\mathcal{F}^{ex}[\rho]}{k_B T}, \quad (\text{S1})$$

where for brevity

$$\sum_i \equiv \sum_{i=1}^6, \quad \sum_\alpha \equiv \sum_{\alpha=1}^M, \quad \int d\mathbf{r} \equiv \int_V d\mathbf{r}.$$

The excess term $\mathcal{F}^{ex}[\rho]$ has in general a non-trivial dependence on $\rho_i^\alpha(\mathbf{r})$. For short-range potentials it is always possible to express $\mathcal{F}^{ex}[\rho]$ as a virial series in the single-particle density. Therefore, by truncating the series at second-virial order and thus disregarding higher-order contributions, one obtains

$$\frac{\mathcal{F}^{ex}[\rho]}{k_B T} = -\frac{1}{2} \int d\mathbf{r} d\mathbf{r}' \sum_{\alpha, \alpha', i, i'} f_{ii'}^{\alpha\alpha'}(\mathbf{r} - \mathbf{r}') \rho_i^\alpha(\mathbf{r}) \rho_{i'}^{\alpha'}(\mathbf{r}'), \quad (\text{S2})$$

where the Mayer function $f_{ii'}^{\alpha\alpha'}(\mathbf{r})$ is defined in terms of the pairwise interaction potential $u_{ii'}^{\alpha\alpha'}(\mathbf{r})$ as

$$f_{ii'}^{\alpha\alpha'}(\mathbf{r}) = \exp\left[-\frac{u_{ii'}^{\alpha\alpha'}(\mathbf{r})}{k_B T}\right] - 1. \quad (\text{S3})$$

The single-particle density $\rho_i^\alpha(\mathbf{r})$ is related to the number of particles N_α through the normalization condition

$$\int d\mathbf{r} \sum_i \rho_i^\alpha(\mathbf{r}) = N_\alpha = x_\alpha N. \quad (\text{S4})$$

For hard cuboids the interaction potential, which expresses the impenetrability of the particles, is

$$\frac{u_{ii'}^{\alpha\alpha'}(\mathbf{r})}{k_B T} = \begin{cases} \infty & \text{if } |x| < (X_i^\alpha + X_{i'}^{\alpha'}) \\ & \text{and } |y| < (Y_i^\alpha + Y_{i'}^{\alpha'}) \\ & \text{and } |z| < (Z_i^\alpha + Z_{i'}^{\alpha'}); \\ 0 & \text{otherwise.} \end{cases} \quad (\text{S5})$$

According to the index notation defined in Tab. S1, the 6-dimensional vectors \mathbf{X}^α , \mathbf{Y}^α and \mathbf{Z}^α of species α are given in terms of the dimension of the particles by

$$\begin{aligned} \mathbf{X}^\alpha &= \frac{1}{2}(L_\alpha, W_\alpha, T_\alpha, L_\alpha, W_\alpha, T_\alpha), \\ \mathbf{Y}^\alpha &= \frac{1}{2}(W_\alpha, T_\alpha, L_\alpha, T_\alpha, L_\alpha, W_\alpha), \\ \mathbf{Z}^\alpha &= \frac{1}{2}(T_\alpha, L_\alpha, W_\alpha, W_\alpha, T_\alpha, L_\alpha). \end{aligned} \quad (\text{S6})$$

The main goal of this work is to study the stability of spatially homogeneous phases (i.e. isotropic and nematic). In order to simplify the problem we therefore neglect spatial modulations in the single-particle density by imposing $\rho_i^\alpha(\mathbf{r}) = \rho_i^\alpha$. Consequently, Eq. (S1) becomes

$$\frac{\mathcal{F}}{V k_B T} = \sum_{\alpha, i} \rho_i^\alpha \left[\ln(\rho_i^\alpha \Lambda_\alpha^3) - 1 \right] + \frac{1}{2} \sum_{\alpha, \alpha', i, i'} E_{ii'}^{\alpha\alpha'} \rho_i^\alpha \rho_{i'}^{\alpha'}, \quad (\text{S7})$$

which is the restricted orientation version of the Onsager free energy [3]. The matrix $E_{ii'}^{\alpha\alpha'}$ in Eq. (S7) is the excluded volume between two particles belonging to species

α and α' with orientations i and i' interacting through the potential Eq. (S5)

$$E_{ii'}^{\alpha\alpha'} = 8(X_i^\alpha + X_{i'}^{\alpha'})(Y_i^\alpha + Y_{i'}^{\alpha'})(Z_i^\alpha + Z_{i'}^{\alpha'}). \quad (\text{S8})$$

In the homogeneous case the normalization condition Eq. (S4) becomes

$$\sum_i \rho_i^\alpha = x_\alpha n. \quad (\text{S9})$$

The single-particle density at equilibrium is the one which minimizes Eq. (S7) with the constraints of Eq. (S8) for all $\alpha = 1, \dots, M$, hence it is found by solving the Euler-Lagrange equation

$$\rho_i^\alpha = \frac{x_\alpha n \exp\left(-\frac{1}{2} \sum_{\alpha', i'} E_{ii'}^{\alpha\alpha'} \rho_{i'}^{\alpha'}\right)}{\sum_{i''} \exp\left(-\frac{1}{2} \sum_{\alpha', i'} E_{ii''}^{\alpha\alpha'} \rho_{i''}^{\alpha'}\right)}, \quad (\text{S10})$$

which is achieved by standard numerical (iterative) techniques.

II. NEMATIC-SMECTIC BIFURCATION

While studying the homogeneous equilibrium phases of the system, we are also interested in estimating their upper bound in the phase diagram, where spatially inhomogeneous phases tend to be thermodynamically favored. Bifurcation theory [4, 5] provides a way to investigate the limit of stability of a particular phase.

The condition of thermodynamic stability of a phase described by the single-particle density $\rho_i^\alpha(\mathbf{r})$ requires that the system corresponds to a minimum of the free energy \mathcal{F} , i.e. a stationary point that satisfies

$$\int d\mathbf{r} d\mathbf{r}' \sum_{\alpha, \alpha', i, i'} \frac{\delta^2 F}{\delta \rho_i^\alpha(\mathbf{r}) \delta \rho_{i'}^{\alpha'}(\mathbf{r}')} \delta \rho_i^\alpha(\mathbf{r}) \delta \rho_{i'}^{\alpha'}(\mathbf{r}') > 0, \quad (\text{S11})$$

for any arbitrary perturbation $\delta \rho_i^\alpha(\mathbf{r})$. By inserting the functional expression Eq. (S1) into Eq. (S11), one finds that the reference phase (described by $\rho_i^\alpha(\mathbf{r})$) ceases to be stable at the smallest density $n = N/V$ at which a perturbation $\delta \rho_i^\alpha(\mathbf{r})$ exists such that

$$\delta \rho_i^\alpha(\mathbf{r}) = \rho_i^\alpha(\mathbf{r}) \int d\mathbf{r}' \sum_{\alpha', i'} f_{ii'}^{\alpha\alpha'}(\mathbf{r} - \mathbf{r}') \delta \rho_{i'}^{\alpha'}(\mathbf{r}'). \quad (\text{S12})$$

Here we are interested in calculating the limit of stability of the (uniaxial or biaxial) nematic phase with respect to smectic fluctuations. With this in mind, in Eq. (S12) we neglect spatial modulations in the reference phase, i.e.

$\rho_i^\alpha(\mathbf{r}) = \rho_i^\alpha$, and a positional dependence of the fluctuations only along the z direction, i.e. $\delta \rho_i^\alpha(\mathbf{r}) = \delta \rho_i^\alpha(z)$. After some rearranging Eq. (S12) becomes

$$\sigma_i^\alpha(z) = \sum_{\alpha', i'} \int dz' Q_{ii'}^{\alpha\alpha'}(z - z') \sigma_{i'}^{\alpha'}(z'), \quad (\text{S13})$$

where $\sigma_i^\alpha(z) = \delta \rho_i^\alpha(z) / \sqrt{\rho_i^\alpha}$ and

$$Q_{ii'}^{\alpha\alpha'}(z) = \sqrt{\rho_i^\alpha \rho_{i'}^{\alpha'}} \int dx dy f_{ii'}^{\alpha\alpha'}(\mathbf{r}), \quad (\text{S14})$$

a symmetric (Hermitian) kernel. By inserting the explicit form of the inter-particle potential (cf. Eq. (S3) and (S5)) into Eq. (S14), we obtain

$$Q_{ii'}^{\alpha\alpha'}(z) = \begin{cases} -4\sqrt{\rho_i^\alpha \rho_{i'}^{\alpha'}} (X_i^\alpha + X_{i'}^{\alpha'}) (Y_i^\alpha + Y_{i'}^{\alpha'}) & \text{if } |z| < (Z_i^\alpha + Z_{i'}^{\alpha'}); \\ 0 & \text{otherwise.} \end{cases} \quad (\text{S15})$$

Eq. (S13) can be more conveniently solved in Fourier space, where it reads

$$\hat{\sigma}_i^\alpha(q) = \sum_{\alpha', i'} \hat{Q}_{ii'}^{\alpha\alpha'}(q) \hat{\sigma}_{i'}^{\alpha'}(q), \quad (\text{S16})$$

with

$$\hat{Q}_{ii'}^{\alpha\alpha'}(q) = -\sqrt{\rho_i^\alpha \rho_{i'}^{\alpha'}} E_{ii'}^{\alpha\alpha'} j_0(q(Z_i^\alpha + Z_{i'}^{\alpha'})), \quad (\text{S17})$$

and $j_0(x) = \sin(x)/x$.

In conclusion, the limit of stability of the nematic phase with respect to smectic fluctuations can be numerically found as the minimum packing fraction η^* at which there exists a wave vector q^* such that the $6M \times 6M$ matrix with entries $\hat{Q}_{ii'}^{\alpha\alpha'}(q^*)$ has a unit eigenvalue. The periodicity of the corresponding bifurcating smectic phase is given by $\lambda^* = 2\pi/q^*$.

III. NEARLY SECOND-ORDER CHARACTER OF THE IN_\pm TRANSITION

When dealing with mixtures, the phase diagram is conveniently expressed in terms of the osmotic pressure P vs. the mole fraction x_α of $M - 1$ components. In this way it is possible to visualize the coexistence of phases characterized by a different composition with respect to the parent distribution. This phenomenon, called demixing or fractionation, is a consequence of the first-order character of the transition.

Here we analyze demixing in a binary mixture of cuboids parameterized as in Eq. (3) with $L/T = 9.07$,

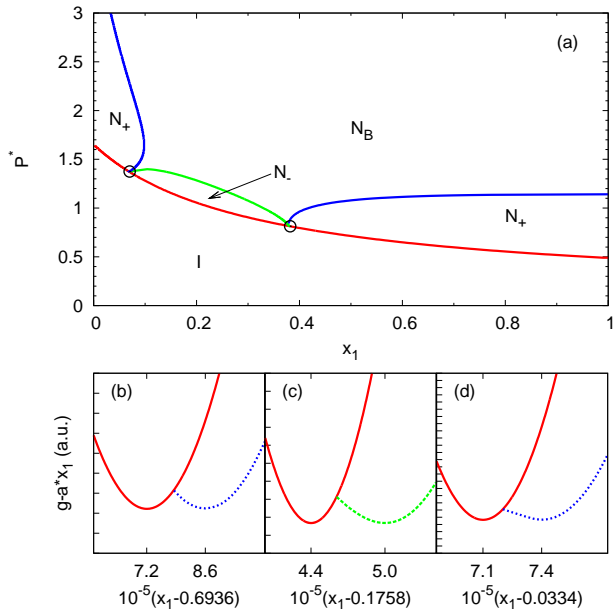


FIG. S1. (a) Phase diagram of a binary mixture of hard cuboids in terms of the reduced osmotic pressure $P^* = PLWT/(k_B T)$ vs. mole fraction of the first species x_1 . (b)-(d) I (red solid line), N_+ (blue dotted line) and N_- (green dashed line) branches of the Gibbs free energy per particle $g = G/N$ at (b) $P^* = 0.6$, (c) $P^* = 1.1$ and (d) $P^* = 1.5$. A straight line with slope $a = \partial g / \partial x_1|_{x_1=x_I} = \partial g / \partial x_1|_{x_1=x_N}$ (with x_I and x_N the compositions of the coexisting isotropic and nematic phases) was subtracted in each case to enhance the visualization of the common tangent construction.

$W/T = 2.96$ and $s = 0.2$. In Fig. S1(a) we report the phase diagram for such a system as a function of the mole fraction x_1 of the larger species. The expected first-order character of the IN_U transitions is not detectable at this scale (see below), whereas the $N_U N_B$ transitions appear to be second order. At three different values of the reduced pressure $P^* = PLWT/(k_B T)$ we calculated the isotropic and uniaxial nematic branches of the Gibbs free energy per particle $g(P, x_1) = G(P, N_1, N_2)/(k_B T(N_1 + N_2))$. The coexistence between the two phases is given by a common tangent construction, which allows to evaluate the difference in composition Δx_1 of the coexisting phases. The results are reported in Fig. S1(b)-(d) for $P^* = 0.6, 1.1$ and 1.5 , respectively. In the three cases, two of which describe a IN_+ and one a IN_- transition, $\Delta x_1 \approx 10^{-5}$ and can therefore be neglected. The situation does not change when one considers different values of the bidispersity parameter s .

Although Landau-de Gennes theory predicts the IN_U transition to be first order [6], we have just shown that its discontinuous character can be safely neglected for the binary mixture of boardlike particles we consider in this work. In our opinion, this fact is tightly related to the shape of the particles close to the $\nu = 0$ value. In fact, when considering a monodisperse system, the closer

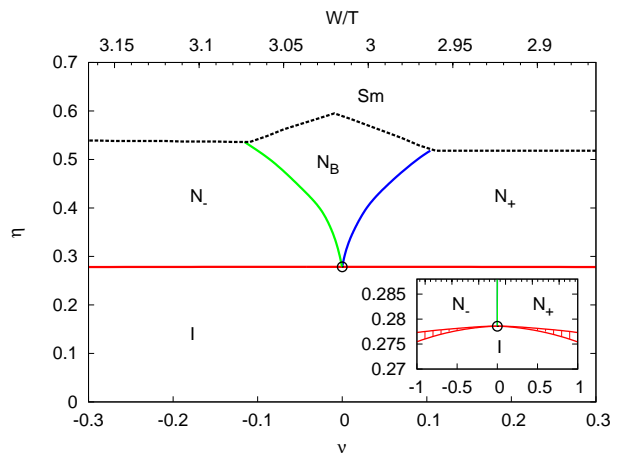


FIG. S2. Phase diagram of a monodisperse system of hard cuboids as a function of the shape parameter $\nu = L/W - W/T$ (with $L/T = 9.07$ fixed and W/T variable). The solid lines indicate phase boundaries as calculated by minimizing the Onsager-Zwanzig functional, the dashed line indicates the limit of stability of the nematic with respect to the smectic phase and the open circle the Landau tetracritical point. The inset highlights the first order character of the IN_U transition and how this tends to become continuous by approaching $\nu = 0$.

ν is to zero the weaker is the first-order character of the IN_U transition (see also Sec. IV). This fact allows us to assume that for an arbitrary number of components of volume-polydisperse cuboids close to $\nu = 0$ the IN_U transition can be approximated as continuous. As a consequence, we can neglect demixing in the phase behavior analysis reported in Fig. 4, thus reducing enormously the complexity of the problem.

IV. MONODISPERSE SYSTEM OF HARD CUBOIDS

The main goal of the present work is to investigate how polydispersity affects the phase behavior, and in particular the stability, of the N_B phase in a system of hard cuboids. For this reason, it is instructive to study what the theoretical framework described in Sec. I predicts in the monodisperse case $M = 1$. In particular, we will focus here on the role of the particles dimensions on the phase behavior of the system.

In Fig. S2 we report the phase diagram of a monodisperse system of hard cuboids as a function of the aspect ratio W/T at fixed $L/T = 9.07$. Consequently, by varying W/T one varies the shape parameter $\nu = L/W - W/T$, in such a way that by crossing the point $\nu = 0$ one expects a transition from plate- to rod-like behavior. This is precisely what Fig. S2 shows, where the phase separation lines are calculated by minimizing the Onsager-Zwanzig functional Eq. (S7) with the constraint of Eq. (S9) for each value of the packing fraction

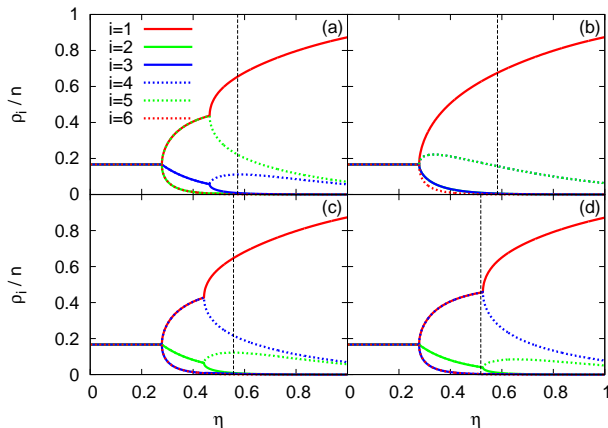


FIG. S3. Orientation distribution function of a monodisperse system of hard cuboids as a function of the packing fraction η obtained by minimization of the Onsager-Zwanzig functional Eq. (S7) for $M = 1$. The cuboids have dimensions $L/T = 9.07$ and (a) $W/T = 3.04$, (b) $W/T = 3.01$, (c) $W/T = 2.99$, (d) $W/T = 2.96$. The different lines indicate the probability of a particular orientation $i = 1, \dots, 6$ (cf. Tab. S1). The dashed vertical line shows the limit of stability of the nematic phases with respect to the smectic.

η . Moreover, bifurcation theory (cf. Sec. II) provides a way to estimate the upper limit of stability of homogeneous phases with respect to the smectic (dashed line in Fig. S2). Fig. S2 shows that to observe a stable N_B phase, the shape of the particles should be designed with extremely high precision in a small ν -regime about $\nu = 0$. In fact, for $L = 9.07T$ the N_B phase disappears unless $2.96T < W < 3.08T$. This is due both to the tight cusp-like shape of the N_UN_B transition line and to the preempting character of inhomogeneous phases. Analogous results can be obtained by varying the shape parameter through L/T , while keeping W/T fixed (not shown). Finally, in the inset of Fig. S2 (note the different scale) we show the first order character of the IN_U transition, which tends to become second-order by approaching the critical point at $\nu = 0$.

For the sake of completeness, in Fig. S3 we report the orientation distribution function p_i , which is the proba-

bility of a given orientation $i = 1, \dots, 6$ as a function of the packing fraction η for different values of the shape parameter ν . In the monodisperse case this function coincides with the single-particle density divided by the number density: $p_i = \rho_i/n$. The values of the orientation distribution function characterize the symmetry of the corresponding phase. In fact, at a given packing fraction η in Fig. S3 one can have one of the following possibilities:

- the probabilities p_i are all the same, i.e. $p_i = 1/6$ (isotropic I phase);
- the probabilities p_i are coupled two-by-two, demonstrating the presence of a symmetry axis (uniaxial nematic N_U phase);
- the probabilities p_i are different between each others (biaxial nematic N_B phase).

Moreover, in the uniaxial nematic case one can further distinguish two situations:

- ▲ the two more probable orientations have the shortest axis aligned along the same direction (uniaxial nematic oblate N_- phase);
- ▲ the two more probable orientations have the longest axis aligned along the same direction (uniaxial nematic prolate N_+ phase).

This classification is easily generalized to the multi-component case. With this in mind, one can observe the difference in the orientation distribution function when $\nu = -0.06 < 0$ ($W/T = 3.04$, Fig. S3(a)), $\nu = 0$ ($W/T = 3.01$, Fig. S3(b)) and $\nu = 0.04 > 0$ ($W/T = 2.99$, Fig. S3(c)). The vertical dashed line indicates the limit of stability with respect to smectic fluctuations as given by bifurcation theory. Finally, Fig. S3(d) shows the predicted orientation distribution function when the experimental value $W/T = 2.96$ is considered [7], and highlights how according to the model the N_B phase is expected to be preempted by inhomogeneous phases.

[1] R. Zwanzig, J. Chem. Phys. **39**, 1714 (1963).
 [2] R. Evans, Adv. Phys. **28**, 143 (1979).
 [3] L. Onsager, Ann. N.Y. Acad. Sci. **51**, 627 (1949).
 [4] R. F. Kaiser and H. J. Raveché, Phys. Rev. A **17**, 2067 (1978).

[5] B. Mulder, Phys. Rev. A **35**, 3095 (1987).
 [6] P. G. de Gennes and J. Prost, *The Physics of Liquid Crystals* (Clarendon, Oxford, 1993).
 [7] E. van den Pol et al., Phys. Rev. Lett. **103**, 258301 (2009).